Battlefield Target Localization Using Acoustic Vector Sensors and Distributed Processing *

Malcolm Hawkes   *Arye Nehorai*

EECS Department (M/C 154)
The University of Illinois at Chicago
851 S. Morgan St
Chicago, IL 60607
Email: hawkes@eecs.uic.edu and nehorai@eecs.uic.edu
URL: *http://www.eecs.uic.e du/~hawkes/* and *http://www.eecs.uic.e du/~nehorai/*

Abstract

We deriv eand analyze fast wideband algorithms for locating airborne targets using a passiv e acoustic sensor system. The system consists of a distributed array of a small, lightweight acoustic v ector sensors, either located in fixed positions on the battlefield or carried by individual soldiers. These sensors measure the acoustic pressure and all three components of particle velocity at a single point — the use of such sensors, which have numerous advan tages o ver traditional pressure sensors, has recently become possible with the development of a new air-based particle velocity sensor now available commercially. We deriv e a bearing-only estimator based on estimation of the acoustic intensity vector applicable to single vector sensor. The estimator provides a local estimate of target bearing without the need for in ter-sensor communication, which is useful if the sensor is carried b y a battlefield unit, for example.. We then develop a 3-D location estimator by combining the local bearing estimates at a central processor. We also calculate an optimal performance measure for the local bearing based on the Cramér-Rao bound and use it to assess the full potential of our distributed array concept and the efficiency of our algorithms. Numerical simulations are used to show the effectiveness of our solutions.

Form SF298 Citation Data

Report Date ("DD MON YYYY") 00001999	Report Type N/A	Dates Covered (from... to) ("DD MON YYYY")

Title and Subtitle		Contract or Grant Number
Battlefield Target Localization Using Acoustic Vector Sensors and Distributed Processing		
		Program Element Number

Authors		Project Number
Hawkes, Malcolm Nehorai, Arye		
		Task Number
		Work Unit Number

Performing Organization Name(s) and Address(es)	Performing Organization Number(s)
EECS Department (M/C 154) The University of Illinois at Chicago 851 S. Morgan St Chicago, IL 60607	

Sponsoring/Monitoring Agency Name(s) and Address(es)	Monitoring Agency Acronym
	Monitoring Agency Report Number(s)

Distribution/Availability Statement
Approved for public release, distribution unlimited

Supplementary Notes

Abstract

Subject Terms

Document Classification unclassified	Classification of SF298 unclassified
Classification of Abstract unclassified	Limitation of Abstract unlimited

Number of Pages 18	

1 Introduction

Acoustic emissions from battlefield sources can provide an invaluable signature by which to detect, locate, and track hostile tanks, trucks, helicopters, and sniper positions that are camouflaged or have low radar cross sections. In addition, the passivity of an acoustic surveillance system allows it to monitor the battlefield without giving away its own presence. A number of researchers have considered the use of arrays of pressure sensors (ordinary microphones) to perform this function [1]–[5] and have demonstrated the feasibility of battlefield acoustic localization and tracking.

We propose to consider the use of *acoustic vector sensors* (AVS's), both individually and elements of an array, to perform the above battlefield surveillance functions. These sensors measure the (scalar) acoustic pressure and all 3 components of the acoustic particle velocity vector at a given point. They have been shown to possess a number of advantages over arrays of standard pressure sensors that would make them especially valuable on the battlefield, in both unattended and mobile system contexts. These advantages arise because AVS's extract source information present in the structure of the velocity field that an array of standard pressure sensors cannot. For example, the direction of the particle velocity vector in a planewave or spherical wave coincides with the line from sensor to source. This extra information, above and beyond a simple increase of signal-to-noise ratio (SNR), is what gives AVS's and AVS arrays their particular advantages over traditional pressure-only systems.

The use of these sensors was first considered from an analytical point of view in [6], [7] for the localization of far-field sources and further studied in [8] and [9]. A number of estimation algorithms have also been derived [10] and [11]. From a practical perspective vector sensors have already been constructed [12] and tested [14], [12]–[16]. Inherent to the current problem is the presence of a reflecting boundary — the ground — near the sensors. The use of vector sensors near a boundary has been analyzed in [17]–[19], and they have been tested on a mock vessel hull [20] and at the seabed [21].

Until now vector-sensor research has been directed to underwater situations. However recently a new aero-acoustic probe called the Microflown, has become commercially available, from Microflown Technologies, B.V. [22] in the Netherlands. This probe is a micro-machined sensor that measures the differential resistance between two heated cantilevers in an airflow and its output is directly proportional to acoustic pressure [23], [24]. These sensors are currently available individually or packaged with a pressure microphone to form a single axis intensity probe. We propose combining three orthogonally oriented Microflowns with a pressure sensor in a single package to create an aero-acoustic vector sensor. As the probe is micro-machined the resultant package would be a very lightweight sensor an amenable to being carried by an individual soldier.

In this paper we develop decentralized processing algorithms for locating airborne acoustic sources using a single vector sensor and using a distributed array over arbitrarily placed vector sensors located on the surface of the ground. The algorithms are applicable to either a fixed array of unattended or a dynamic array of mobile sensors carried by individual soldiers or other battlefield units.

A decentralized algorithm is one in which some processing is carried out locally in subarrays before being combined centrally. In our algorithm the subarrays consist of individual vector sensors that independently estimate the local bearing from their location to the target. The bearing estimate

is derived from estimates of the three components of the local intensity vector. An estimate is also made of its variability. While this information is of use to the soldier carrying the unit in its own right it can also be transmitted to a central processor along with its variability estimate. We then propose to use a weighted least-squares (WLS) techniques to combine the various bearing estimates into a single 3-D estimate of the target's location. As a variation we also propose a re-weighted LS method, to account for the different ranges of the sensors from the target. We analyze the local bearing estimator by deriving an optimal bound on its mean-square angular error (MSAE) for comparison.

Any decentralized processor is suboptimal since it does not make use of the correlations between sensors at different locations, it has a number of practical advantages. Firstly each sensor is small enough to be carried by an individual soldier which makes it a very flexible system. There are no restrictions on the placement of sensors they may be arbitrarily far apart, and need not possess any particular geometrical structure. This is an essential characteristic as the geometrical demands of an array processing regime cannot be a deciding factor in a unit's placement in a hostile environment. Furthermore, each sensor is able to provide a bearing estimate of the source to the unit carrying it without the need to communicate with others sensor or the central processor so not exposing itself to detection. Even when communication is made to the central processor, minimal data need to be sent, merely the bearing estimate, an estimate of its accuracy, and the sensor's current location. This compares very favorably with a fully optimal design which would require every sensor to transmit every sample of every component, thereby greatly increasing the risk of detection as well as computational overhead. Lastly, the algorithms for local bearing estimation and global position estimation are both inherently wideband algorithms and also very computationally efficient as they require no numerical optimization. Thus estimates can be obtained very rapidly, which is almost a *de-facto* requirement of localizing airborne targets, with minimal hardware costs.

In theory we could replace each vector sensor with a small array of distributed pressure sensors and use the same decentralized processing methodology, in fact decentralized algorithms for sub-arrays of omni-directional sensors have been proposed and analyzed for far-field [25] and near-field [26]. However, this would require greater computational costs because a numerical optimization procedure would be required at each array. In addition, the minimum frequency of interest in airborne applications is 50Hz (see discussion in Section 5) and so each individual array would be incredibly cumbersome to transport if it were to be large enough to attain any reasonable degree of accuracy. Therefore the use of vector sensors is essential to the development of the flexible system we ere propose.

In Section 2 we epresent the mathematical model for the sensor measurements, Section 3 develops an algorithm to rapidly estimate bearing using a single vector sensors. In Section 4 we develop weighted and re-weighted least-squares algorithms for determining 3-D aircraft position given the bearing estimates from each sensor, construct an estimator to determine the weights, and give an expression for a lower bound on the bearing estimator from each sensor. Section 5 provides numerical examples and Section 6 concludes. Extensions are presented in Section 7.

2   Measurement Model

We assume that there is a single airborne acoustic source radiating spherical waves whose signal is received my m vector sensors at arbitrary distinct locations on a flat ground surface.

If the source is not too close to the boundary, the field due to a point source can be obtained by creating a point image source, obtained by reflecting the source in the boundary and with amplitude and phase determined by the boundary characteristics, then summing the fields from the two sources as if the boundary werenot present. Note that if the source is very close to the boundary, ground waves and surface waves may exit [34]. The resultant field may still be obtained using an image source for locally reacting surfaces but now the image source must be somewhat modified [29]. However, we shall not consider that case in the present paper.

Assume, therefore, that the point source is far enough away from ground that the resulting field can be regarded as arising from point source radiating spherically symmetric waves and simple point image, therefore ground waves and surfaces wavesdo not exist. This is the case for an airborne source. The pressure and radial velocity my be described in terms of the velocity potential, which for a spherically symmetric wave is

$$\Phi(r,t) = F(t - r/c)/r\,, \tag{2.1}$$

where r is the distance from the source, c is the sound speed, and $F(\cdot)$ is an arbitrary differentiable function. The pressure and radial velocity are then [30]

$$p(r,t) = \frac{\partial \Phi(r,t)}{\partial t} \tag{2.2}$$

$$v_r(r,t) = -\frac{1}{\rho_0}\frac{\partial \Phi(r,t)}{\partial r}, \tag{2.3}$$

respectively. Therefore

$$p(r,t) = \frac{f'(t - r/c)}{r} \tag{2.4}$$

$$v_r(r,t) = \frac{p(r,t)}{\rho_0 c} + \frac{F(t - r/c)}{\rho_0 r^2}, \tag{2.5}$$

where $f'(\cdot)$ is the derivativ eof $F(\cdot)$. Since the second term in (2.5) decreases as $1/r^2$ while the first goes down as $1/r$, it is negligible at distances of more than a few wavelengths. The minimum frequency of interest in aircraft location is about 50Hz corresponding to about 6.6m (see discussion in Section 5), so we shall ignore it.

Suppose we hav ean airborne source located at a distance r and (unit length) bearing vector $\boldsymbol{u}$ from a sensor located on the ground, which defines the x, y-plane; the $z - axis$ is taken to point upward. Construct an image source by reflecting the source in the x, y-plane that also radiates the spherical wave but with different amplitude and phase, i.e. if $\Phi(r,t)$ represents the phasor notation (also known as the complex env elope or analytic signal) of the source field's velocity potential, the image source has velocity potential $\mathcal{R}\Phi(r,t)$, where $\mathcal{R}$ is complex. Therefore the complex env elopes of the pressure and velocit y fields at the sensor are

$$p(t) = \tilde{p}(t)(1 + \mathcal{R}) \tag{2.6}$$

$$\boldsymbol{v}(t) = -\frac{1}{\rho_0 c}(\boldsymbol{u} + \mathcal{R}\boldsymbol{u}_{\text{image}})\tilde{p}(t), \tag{2.7}$$

where $\tilde{p}(t)$ is the complex env elope of $f'(t - r/c)/r$, $\boldsymbol{u}$ is the unit vector pointing from the sensor to the (real) source, and $\boldsymbol{u}_{\text{image}}$ is obtained from $\boldsymbol{u}$ by negating the$z$-component. The presence of the

boundary imposes the condition $-p(t)/v_z(t) = Z_{\text{in}}$ at $z = 0$ [30], where $v_z(t)$ is the z-component of $\boldsymbol{v}(t)$, and Z_{in} is the specific acoustic impedance of the surface. Therefore

$$Z_{\text{in}} = -\frac{(1+\mathcal{R})\rho_0 c}{\sin\psi(1-\mathcal{R})}, \tag{2.8}$$

where ψ is the elevation of the source with respect to the sensor. Therefore

$$\mathcal{R} = \frac{Z_{\text{in}} - \rho_0 c/\sin\psi}{Z_{\text{in}} + \rho_0 c/\sin\psi}. \tag{2.9}$$

The quantity $\mathcal{R}$ is known as the reflection coefficient. In general Z_{in} is a function, possibly quite complex, of ψ, or equivalently the incidence angle $\gamma = pi/2 - \psi$, and frequency. How ever, [34] concluded that various ground surfaces behave as if they are locally reacting. A locally reacting surface is one for which Z_{in} is independent of the incidence angle (but not necessarily frequency) and often also arises in architectural acoustics with porous sound-absorbing materials [30]. A locally reacting surface may be characterized as one in which the sound disturbance transmitted into the lower medium does not travel along its boundary (actually this is only strictly true for plane waves since, as mention above, ground waves and surface waes may exist when the source is very close to the boundary) and therefore the normal velocity at each point is completely determined by the pressure at this point [31].

It follo ws from the above development that the measurement of a single vector sensor at bearing $\boldsymbol{u}$ from the source may be written as a complex four-element vector

$$\boldsymbol{y}(t) \triangleq \begin{bmatrix} y_p(t) \\ \boldsymbol{y}_v(t) \end{bmatrix} = \boldsymbol{h}\tilde{p}(t) + \boldsymbol{e}(t) \qquad t = 1, 2, \ldots, \tag{2.10}$$

where $y_p(t)$ is the pressure measurement $\boldsymbol{y}_v(t)$ contains the three orthogonal velocity measurements, $\boldsymbol{e}(t)$ represents noise, and $\boldsymbol{h}$, the steering vector is given by

$$\boldsymbol{h} = \begin{bmatrix} 1+\mathcal{R} \\ (1+\mathcal{R})\cos\phi\cos\psi \\ (1+\mathcal{R})\sin\phi\cos\psi \\ (1-\mathcal{R})\sin\psi \end{bmatrix}, \tag{2.11}$$

where ϕ is the source's azimuth relative to the sensor. The expression (2.11) for $\boldsymbol{h}$ assumes that the three velocit ycomponents are aligned withe three coordinate axes, or that the orientation of the sensor is known and that the data ha v ebeen rotated to achieve the same effect. It should not be difficult to design a sensor package for which it is easy talign the v ertical component. T o correctly align the horizontal components a compass would probably have be included in the sensor package, either one that could be aligned b y ey e or, for sensors air-dropped onto a battle field, a digital compass whose output used to rotate the data. Such an idea is used in the underwater vector sensors described in [14]. The measurements are again complex envelopes. Note that the complex envelope of a bandpass signal $x(t)$ is given by $x_i(t) + ix_q(t)$, where $x_i(t)$ and $x_q(t)$ are the in-phase and quadrature component of $x(t)$ respectively (see e.g. [32]).

We assume that the signal and noise processes $\tilde{p}(t)$ and $\boldsymbol{e}(t)$ are zero-mean uncorrelated processes with finite second order moments and that

$$\text{E}\{\tilde{p}(t)\tilde{p}(\tau)^*\} = \sigma_s^2 \delta_{t,\tau} \tag{2.12}$$

$$\text{E}\{\boldsymbol{e}(t)\boldsymbol{e}(\tau)^H\} = \sigma^2 I \delta_{t,\tau}, \tag{2.13}$$

where $\delta_{t,\tau}$ is the Kronecker delta function, I is the identity matrix, the superscript * represents conjugation and superscript ^{H} complex conjugation and transposition. In fact the assumption of independent time samples is not strictly necessary for the following algorithms to be implemented. If there is time correlation, however more samples will be required to achieve a given level of accuracy.

To calculate the performance measure for the bearing-only estimator and to implement the simulations we will make the further assumption that both processes are Gaussian. If, for example, the signal and noise processes are band-limited Gaussian stochastic processes, with power spectral densities that are symmetrical about the center frequency, then the complex envelopes will satisfy the above assumptions if they are sampled at the Nyquist rate, i.e. twice the bandwidth.

Now suppose there are m sensors located at $\boldsymbol{r}_1, \dots \boldsymbol{r}_m$, and denote the 3-D source location vector by $\boldsymbol{\theta}$. Letting $\tilde{p}(t)$ be the pressure signal at the origin, the total measurements from the array are then

$$\boldsymbol{y}_i(t) = \boldsymbol{h}(\boldsymbol{u}_i)\frac{\|\boldsymbol{\theta}\|}{\|\boldsymbol{\theta} - \boldsymbol{r}_i\|}\tilde{p}(t - \tau_i) + \boldsymbol{e}_i(t) \qquad i = 1, \dots, m, \; t = 1, 2, \dots \qquad (2.14)$$

where the $\boldsymbol{u}_i$ are the sensor to source bearing vectors and $\tau_i = (\|\boldsymbol{\theta} - \boldsymbol{r}\| - \|\boldsymbol{\theta}\|)/c$ is the differential time delay with respect to the origin. In addition to the above statistical assumptions (2.13) we also assume that the noise processes are uncorrelated from one location to another for the purposes of simulation, but this is not required for the algorithms to work. The noise power at different sensor locations may also vary. Note that we do not account for relative Doppler effects in this model or in our simulations, however, our estimation schemes do not use this information and will work just as well whether it is present or not.

In the following section we derive an algorithm to estimate each of the $\boldsymbol{u}_i$ locally at each vector sensor and in Section 4 we develop a method to combine these estimates to estimate $\boldsymbol{\theta}$.

3 Local Bearing Estimation

In this section we derive a fast wideband algorithm to estimate the bearing of the source $\boldsymbol{u}$ from a single vector sensor. In the mobile array paradigm, where each sensor is carried by a battlefield unit, such as a soldier, this estimate provides vital information the the unit without the need for any communication, thereby not exposing the unit to detection. Acoustic intensity is a vector quantity defined as the product of pressure and velocity. Since the x and y components of the intensity vector are the same for both real and image sources the acoustic intensity vector is parallel to the projection of the source's bearing vector $\boldsymbol{u}$ onto the x, y-plane. Therefore we can use an estimate of the horizontal acoustic intensity to determine the azimuth. Note that [7] used this technique to derive an estimator for the full bearing vector using a vector sensor in free space, however, it cannot be used to find the elevation when the boundary is present.

The horizontal component of acoustic intensity measured by a single vector sensor located a distance d from a reflecting boundary is

$$\boldsymbol{I}_{\mathrm{h}}(t) = y_p(t) \begin{bmatrix} \bar{y}_{v_x}(t) \\ \bar{y}_{v_y}(t), \end{bmatrix}, \qquad (3.15)$$

where the overbar indicates complex conjugation. Thus, for a narrowband or wideband source, as long as the noise at the various sensors is mutually uncorrelated,

$$\mathrm{E}\{\boldsymbol{I}_\mathrm{h}(t)\} = \sigma_s^2 |1 + \mathcal{R}|^2 \cos \psi \begin{bmatrix} \cos \phi \\ \sin \phi \end{bmatrix} \tag{3.16}$$

Since this is purely real we let $\hat{\boldsymbol{s}} = N^{-1} \sum_{t=1}^{N} \mathrm{Re}\{\boldsymbol{I}_\mathrm{h}(t)\}$, and by the strong law of large numbers $\hat{\boldsymbol{s}} \to \mathrm{E}\{\boldsymbol{I}_\mathrm{h}(t)\}$. Thus we can estimate azimuth from

$$\hat{\boldsymbol{u}}_\mathrm{h} \triangleq \begin{bmatrix} \cos \hat{\phi} \\ \sin \hat{\phi} \end{bmatrix} = \frac{\hat{\boldsymbol{s}}}{\|\hat{\boldsymbol{s}}\|} \to \boldsymbol{u}_\mathrm{h} \triangleq \begin{bmatrix} \cos \phi \\ \sin \phi \end{bmatrix} \tag{3.17}$$

Note that equation (3.17) is independent of $\mathcal{R}$, and so we can use this estimator to determine the azimuth even without knowing the local reflective properties of the ground. Since the magnitude of the horizontal component of acoustic intensity strongly depends on the elevation so will the accuracy of this azimuthal estimator. To be precise, by adapting the analysis of [7] to the present scenario, we can show that its asymptotic MSAE is

$$\mathrm{MSAE}(\hat{\boldsymbol{u}}_\mathrm{h}) \triangleq \lim_{N \to \infty} N \, \mathrm{E}(\hat{\phi} - \phi)^2 = \frac{1 + |1 + \mathcal{R}|^2 \rho}{2\rho^2 |1 + \mathcal{R}|^4 \cos^2 \psi}. \tag{3.18}$$

To obtain an estimator of the elevation is somewhat more complicated. First suppose that the input impedance Z_in is approximately constant across the bandwidth (this is the only factor that constrains the bandwidth of our algorithm in any way) and note that the vertical component of acoustic intensity $I_\mathrm{v}(t) \triangleq y_p(t)\bar{y}_{v_z}(t)$ has expected value

$$\mathrm{E}\{I_\mathrm{v}(t)\} = \sigma_s^2 (1 + \mathcal{R})(1 - \bar{\mathcal{R}}) \sin \psi \tag{3.19}$$

Using equation (3.16) we note that

$$\chi \triangleq \frac{\mathrm{E}\{I_\mathrm{v}(t)\}}{\|\mathrm{E}\{\boldsymbol{I}_\mathrm{h}(t)\}\|} = \frac{1 - \bar{\mathcal{R}}}{1 + \bar{\mathcal{R}}} \tan \psi = \frac{\rho c}{\bar{Z}_\mathrm{in} \cos \psi}, \tag{3.20}$$

where the second equality follows from (2.9). The quantity on the right-hand side, χ say, is a function of ψ alone, which we propose to estimate from the statistic

$$\hat{\chi} = \frac{\sum_{t=1}^{N} I_\mathrm{v}(t)}{\|\sum_{t=1}^{N} \mathrm{Re}\{\boldsymbol{I}_\mathrm{h}(t)\}\|}. \tag{3.21}$$

It then remains to solve

$$\hat{\chi} = \frac{1 - \bar{\mathcal{R}}(\hat{\psi})}{1 + \bar{\mathcal{R}}(\hat{\psi})} \tan \hat{\psi} = \frac{\rho c}{\bar{Z}_\mathrm{in} \cos \hat{\psi}}, \tag{3.22}$$

for $\hat{\psi}$. Thus we propose the estimate the elevation from

$$\hat{\psi} = \mathrm{Re}\left\{ \cos^{-1} \left| \frac{\rho c}{\hat{\chi} \bar{Z}_\mathrm{in}} \right| \right\}. \tag{3.23}$$

We choose to take absolute values before the inverse cosine, rather than taking real values or applying the inverse cosine to a complex number, because numerical simulations showed that it

resulted in slightly greater accuracy, particularly for large N. The real value of the inverse cosine is taken to deal with (rare) cases in which the argument is larger than one, in these cases we ensure that $\hat{\psi} = 0$. Note that the expression in (3.23) automatically ensures that the estimated elevation is not negative so incorporating the *a-priori* knowledge than the source lies above ground.

It can be seen from the above that the bearing is estimated via the three components of intensity. Therefore, we could in theory use three orthogonally oriented single-axis intensity probes, Microflown Technologies B.V. already packages its novel sensor with a pressure sensor to form such an intensity probe. Intensity probes are available from other manufacturers such as Brüel and Kjær, although those currently available use two closely spaced pressure sensors, instead of true velocity sensors, to determine the velocity. Such sensors are not considered appropriate for vector-sensor processing [7].

4 Centralized Location Estimation

We now consider the problem of how to combine the decentralized estimates of the target bearings to obtain an estimate of its location. Each sensor transmits its local estimate of the direction from its location to the source $\hat{u}_i$ say as well as its own location r_i. The location could be determined from a lightweight GPS receiver carried along with the sensor. In practice both the local bearing and position will contain errors, however, we shall assume that the bearing estimate is the dominant source of error and ignore possible inaccuracies in the location r_i. Therefore, a total of five quantities (four if all sensors are at the same altitude) need be transmitted, three to describe the location and two for the bearing, no matter how long an observation window is used. This is a huge advantage over a centralized processing scheme in terms of communications overhead where every single data sample from every single sensor must be sent to a central processor.

4.1 Weighted Least Squares

If all the $\hat{u}_i$ were without error the collection of m lines passing through each r_i with direction $\hat{u}_i$ would intersect at the true source position. Therefore, we want to choose the estimate of the source's location $\hat{\theta}$ to be a point that is in some sense closest to all these lines. We shall choose $\hat{\theta}$ so as to minimize a weighted sum of the minimum squared distances from $\hat{\theta}$ to each line. By doing so we will derive a closed form solution for the location estimate so avoiding the need for a complex computational search. Any point along the line defined by the ith sensor's location and bearing estimate is defined by the vector $r_i + \mu_i \hat{u}_i$ for some μ_i. For fixed θ the point of closest approach occurs when $\mu_i = \hat{u}_i^T(\theta - r_i)$, i.e. μ_i is the projection of the vector from r_i to θ onto the direction $\hat{u}_i$. Thus the weighted least squares (WLS) estimate of $\hat{\theta}$ is

$$\hat{\theta} = \operatorname*{argmin}_{\theta} \sum_{i=1}^{m} \| r_i + \hat{u}_i^T(\theta - r_i)\hat{u}_i - \theta \|^2 w_i, \tag{4.24}$$

where w_i is a weight corresponding to the accuracy of each $\hat{u}_i$: the better the accuracy of $\hat{u}_i$, the smaller w_i should be. We shall discuss the choice of weights fully in Section 4.2. Expanding (4.24) and rearranging we obtain

$$\hat{\theta} = \operatorname*{argmin}_{\theta} \sum_{i=1}^{m} \left\{ -2r_i^T(I - \hat{u}_i\hat{u}_i^T)\theta + \theta^T(I - \hat{u}_i\hat{u}_i^T)\theta \right\} w_i, \tag{4.25}$$

where we have dropped terms independent of $\boldsymbol{\theta}$. Note that $(I - \hat{\boldsymbol{u}}_i \hat{\boldsymbol{u}}_i^T)$ is the projection matrix onto the plane orthogonal to $\hat{\boldsymbol{u}}_i$. Differentiating with respect to $\boldsymbol{\theta}$ and setting the result equal to zero gives

$$2 \sum_{i=1}^{m} (I - \hat{\boldsymbol{u}}_i \hat{\boldsymbol{u}}_i^T)(\boldsymbol{r}_i - \hat{\boldsymbol{\theta}}) w_i = 0. \tag{4.26}$$

Hence,

$$\hat{\boldsymbol{\theta}} = \left[\left(\sum_{i=1}^{m} w_i \right) I - \hat{U} W \hat{U}^T \right]^{-1} A \boldsymbol{w}, \tag{4.27}$$

where $\boldsymbol{w} = [w_1, \dots, w_m]^T$, $W = \text{diag}\{\boldsymbol{w}\}$, $\hat{U} = [\hat{\boldsymbol{u}}_1, \dots, \hat{\boldsymbol{u}}_m]$, and

$$A = \left[(I - \hat{\boldsymbol{u}}_1 \hat{\boldsymbol{u}}_1^T)\boldsymbol{r}_1, \dots, (I - \hat{\boldsymbol{u}}_m \hat{\boldsymbol{u}}_m^T)\boldsymbol{r}_m \right]. \tag{4.28}$$

4.2 Choice of Weights

In general the accuracy of the bearing estimates $\hat{\boldsymbol{u}}_i$ will be different from sensor to sensor due to a number of factors. There may be local variations in background noise level or ground reflectivity, signal strength will differ between sensors that are different distances from the source because of spherical spreading loss, and the accuracy of the estimation algorithm may depend on the true $\boldsymbol{u}_i$, which differs between sensors. Thus, it is important for each sensor to transmit a measure of accuracy only with its bearing estimate to the central processor. A very natural measure in this situation is the mean-squared angular error (MSAE) defined as $\text{E}\, \delta_i^2$ where δ_i is the angle between $\boldsymbol{u}_i$ and its estimate. The analysis of our estimator is somewhat complex and no simple expression is known for the MSAE. Although for ground targets, when only azimuth need be estimated, a closed form expression for the MSAE may be found.

Instead of the MSAE itself, we shall use a bound on the MSAE derived in [7], and given by

$$\text{MSAE}_{\text{b}}(\boldsymbol{u}) = N\{\cos^2 \psi \text{CRB}(\phi) + \text{CRB}(\psi)\}, \tag{4.29}$$

where ϕ and ψ are the azimuth and elevation of the source, relative to the sensor, $\text{CRB}(\cdot)$ indicates the Cramér-Rao bound, and N is the number of snapshots. It has been shown that this bound holds for all N for unbiased estimators of a unit length vector $\boldsymbol{u}$ and asymptotically for a much larger class of estimators [27]. In Appendix A we show that the MSAE_{b} is given by

$$\text{MSAE}_{\text{b}} = \frac{1}{2\rho} \left(1 + \frac{1}{\rho \|\boldsymbol{h}\|^2} \right) \left(\frac{\cos^2 \psi}{\|\partial \boldsymbol{h}/\partial \phi\|^2} + \frac{1}{\|\partial \boldsymbol{h}/\partial \psi\|^2 - |(\partial \boldsymbol{h}^H/\partial \psi)\boldsymbol{h}|^2/\|\boldsymbol{h}\|^2} \right). \tag{4.30}$$

The various expression for $\|\boldsymbol{h}\|^2$, $\|\partial \boldsymbol{h}/\partial \psi\|^2$ are also given in Appendix A, from which it way be seen that MSAE_{b} is a function of the SNR ρ and the elevation ψ, but not the azimuth.

Since MSAE_{b} depends on the unknown quantities ρ and ψ we must actually use an estimate of MSAE_{b} by plugging in estimates of the unknowns. The bearing estimator itself already provides us with and estimate of ψ so its remains to estimate ρ. If we knew the maximum-likelihood (ML) estimate of $\boldsymbol{u}$, say $\hat{\boldsymbol{u}}_{\text{ML}}$, then we could use closed form expressions, see e.g. [28], to find the ML

estimates of $\hat{\sigma}^2$ and $\hat{\sigma}_s^2$. Since we don't know $\hat{\boldsymbol{u}}_{\mathrm{ML}}$, we shall use our actual estimate of $\hat{\boldsymbol{u}}$. Therefore we have

$$\hat{\sigma}^2 = \frac{1}{3} \operatorname{Re} \left\{ \operatorname{tr} \left[\left(I - \frac{\hat{\boldsymbol{h}}\hat{\boldsymbol{h}}^H}{\|\hat{\boldsymbol{h}}\|^2} \right) \hat{R} \right] \right\} \tag{4.31}$$

$$\hat{\sigma}_s^2 = \frac{1}{\|\hat{\boldsymbol{h}}\|^4} \hat{\boldsymbol{h}}^H [\hat{R} - \hat{\sigma}^2 I]\hat{\boldsymbol{h}}, \tag{4.32}$$

where $\hat{\boldsymbol{h}} = \boldsymbol{h}(\hat{\boldsymbol{u}})$ and $\hat{R}$ is the sample covariance matrix. So our estimate of the SNR is $\hat{\rho} = \hat{\sigma}_s^2/\hat{\sigma}^2$. Finally, we plug $\hat{\rho}$ and the elevation estimate $\hat{\psi}$ into (4.30) to obtain $\widehat{\mathrm{MSAE}}_{\mathrm{b}}$ and the weight that we will use in determining $\hat{\boldsymbol{\theta}}$ is $1/\widehat{\mathrm{MSAE}}_{\mathrm{b}}$.

4.3 Reweighting

If a sensor is a long way from the source, a small error in its bearing estimate will have a much more dramatic effect upon the resulting estimate of $\boldsymbol{\theta}$ than if the the sensor is very close to the source. Thus, we should also weight terms of the squared error criterion more heavily for sensors that are close to the than those far away. To be precise the contribution of the ith bearing estimate to the squared error criterion is approximately $l_i^2 \delta_i^2$, where l_i is the distance of the source from the ith sensor and δ_i is the angular error of $\hat{\boldsymbol{u}}_i$. If we knew the l_i a-$priori$ we would ideally like to weight each term by $w_i = 1/(l_i^2 \cdot \mathrm{MSAE}(\boldsymbol{u}_i))$.

Although we do not know the l_i, we do have an estimate of them after we have obtained the first estimate of $\boldsymbol{\theta}$ using the angular error weights alone, therefore we propose a reweighted estimator constructed as follows: Find $\boldsymbol{\theta}$ from the above WLS scheme using the angular error weights alone. $w_i = 1/\widehat{\mathrm{MSAE}}_{\mathrm{b}}(\boldsymbol{u}_i)$. Using $\hat{\boldsymbol{\theta}}$, estimate the distances from each sensor to the source as $\hat{l}_i = \|\hat{\boldsymbol{\theta}} - \boldsymbol{r}_i\|$, then construct a reweighted estimate $\hat{\boldsymbol{\theta}}_{\mathrm{R}}$ using the above WLS scheme but now with $w_i = 1/(\hat{l}_i^2 \cdot \widehat{\mathrm{MSAE}}_{\mathrm{b}}(\boldsymbol{u}_i))$.

5 Numerical Examples

We now illustrate by numerical example the performance of the local bearing estimator and global location estimators derived in the previous section. We also suppose that the ground has normalized input impedance $Z_{\mathrm{in}}/(\rho_0 c) = 11 + 13i$, and that it is approximately constant over this frequency band. This corresponds to the value measured in [34] for grass-covered flat ground at 225Hz, the mid-point of the band.

5.1 Local Bearing Estimation

Figure 1 illustrates the performance of the local bearing estimation algorithm via the standard deviation of its squared angular error, i.e. $\sqrt{\mathrm{MSAE}(\boldsymbol{u})}$ and compares it with the bound $\sqrt{\mathrm{MSAE}_{\mathrm{b}}(\boldsymbol{u})}$. The scenario consists of a 20dB source and 350 snapshots, and 500 realizations were used for each incidence angle. Because of the azimuthal invariance of the steering vector $\boldsymbol{h}$ of a single vector sensor located on the ground, all quantities are function of elevation alone.
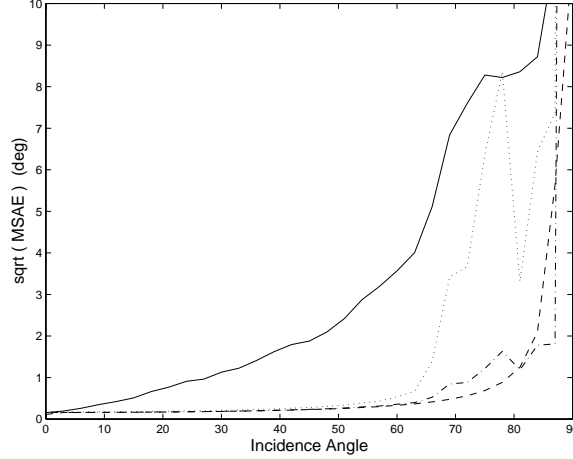
Figure 1: P erformance, in terms of $\sqrt{\text{MSAE}}$, of local bearing estimation algorithm (solid), and bound MSAE_b (dashed), versus incidence angle, for a 20dB source with 350 snapshots. Also shown are the av eraged estimated MSAE_b (dash-dotted) plus three of its empirical standard deviations (dotted). The results were obtained using 500 realizations at each incidence angle.

It can be see that, at normal incidence, our algorithms perfromance reac hesthe MSAE_b but falls off at greater incidence angles, underperforming it by about 8° standard deviation by 80° incidence. This incrseaing lac k of optimality a w ayfrom normal incidence should not hav e too dramatic an effect in practice, how ev eras it seems unlikely that the incidence angle would ever be more than about 45°, even for a low flying aircraft and a very widely spaced array. It can be seen from (2.11) and (2.9), that $|\boldsymbol{h}| \to 0$ as the incidence angle tends towards grazing, leading to v ery low signal levels on all component sensors at large incidence. This is why all curves tend to infintity as w e appraoch grazing.

Not shown in Figure 1 is the standard deviation of the elevation estimate as it essentially follows the curve of the MSAE. Therefore, we conclude that almost all the angular error is due to the error in estimating the elevation and that the error in the azimuthal estimates is negligible in comparison. T o understand this consider Figure 2. It shows the signal gain resulting from reflection at the boundary and the incoming signal's direction for each sensor component, i.e. the squared magnitudes of the en tries of $\boldsymbol{h}$. The pressure sensor gain is seento uniformly larger, because it is omni-directional and is almost flat until shrply tapering off tow ardsgrazing incidence. The in-plane componenet gain (actually it is the gain of the sum of the in-plane components, or equivalently, the gain of one component when $\boldsymbol{u}$ is in the same plane as it axis; this is the quantity of interest because the out put of both sensors together determine the azimuth) is seen to increase aw ayfrom normal, then reach the pressure gain at around 80° before tapering off. It crosses the normal component gain at about 5°. On-the other hand, the normal gain, which determines the ability to estimate elevation, starts off at about -18dB and stays about 24dB below the pressure gain for all angles. The fact that the normal component gain is much low er than both pressure and in-plane gain for most angles explains why the estimate of elevation contributes most of the MSAE. In addition, when the normal gain is larger than the in-plane, v ery near normal incidence, large errors in the azimuthal estimate ha v e little effect on the MSAE because of the inherent singularity in the spherical coordinate system. This poor normal gain is mainly due to the size of the input impedance, if the input impedance w esmall, i.e. the surface were acoustically more pliable, the normal gain would improv e relative
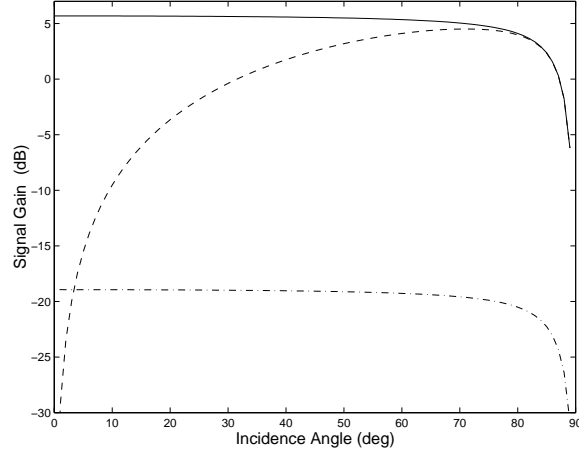
Figure 2: Signal gain resulting from reflection and sensor directionality for pressure (solid), in-plane (dashed), and normal (dash-dotted) components of a vector sensor at a locally reacting boundary. The normalized input impedance is $Z_{\mathrm{in}} = 11 + 13i$.

to the in-plane and pressure gains resulting in better estimation of elevation, but poorer azimuthal estimation.

Also shown in Figure 1 the average estimated bound $\widehat{\mathrm{MSAE}}_{\mathrm{b}}$, which will be used as the weight in the global location estimator, plus 3 standard deviations. The estimate of the $\widehat{\mathrm{MSAE}}_{\mathrm{b}}$, is seen to be very accurate until about 60° and then begins to deviate slightly from the true $\mathrm{MSAE}_{\mathrm{b}}$ and starts to become more variable. It is possible that on any run $\hat{\psi} = 0$, with finite probablility if the argument of the inverse cosine in (3.23) is greater than one. In this case our technique fails to yield an estimate of $\mathrm{MSAE}_{\mathrm{b}}$, beacuse it is theoretically infinite if ψ really is zero as $|\boldsymbol{h}| = 0$, so no signal is present on any of the sensors. In our simulation, this never occurred below 66° incidence, and the chances of it occuring rose to about 50% within a few degrees of grazing incidence. However, as discussed above, we do not expect that such large incidences will need to be measured in this application and so this should not be a problem in practice. If it does occur at one sensor in the array, a solution would be to use the average of the $\widehat{\mathrm{MSAE}}_{\mathrm{b}}$ obtained from the other sensors as the weight the failed sensor.

5.2 Global Location Estimation

We now give an example of the performance of the global location estimator for a wideband signal. Assume that signal arriving at each sensor is a wideband stationary Gaussian signal and that it is bandpass filtered to have spectral support from 50-400Hz. Aircraft noise above this band considerably affected by propagation absorption, while below it, ambient noise (predominantly caused by wind flow wing over the sensors) dominates [4]. The signal is then downsampled with a center frequency 225Hz and the resulting complex envelope sampled at the Nyquist frequency, i.e. twice the bandwidth 700Hz. We assume that the signal and noise power spectra are symmetrical about the center frequency so that the resulting signal and noise samples are i.i.d. complex Gaussian with variance equal to the signal and noise powers respectively.
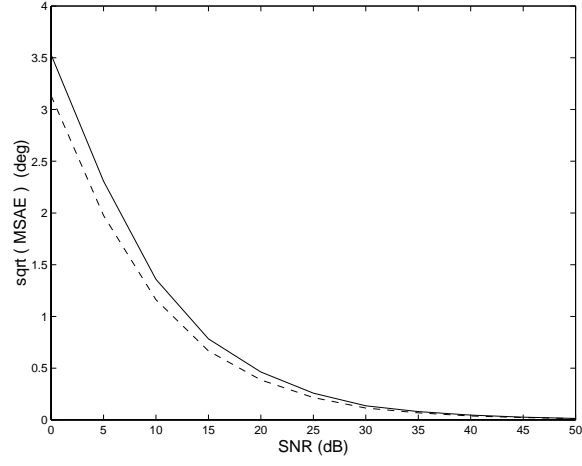
Figure 3: Angular estimation performance in terms of $\sqrt{\mathrm{MSAE}}$ for the WLS and re-weighted LS global location estimators. The scenario is described in the text.
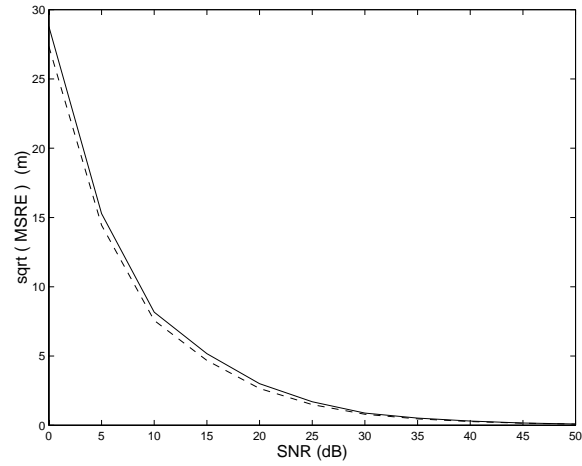

Figure 4: Range estimation performance in terms of $\sqrt{\mathrm{MSRE}}$ for the WLS and re-weigh ted LS global location estimators. The scenario is described in the text.

The source is located at $(4, 5, 100.68)$, and there are six sensors located on the ground with x, y coordinates $(0, 0)$, $(40, 40.52)$, $(20, 18)$, $(40, -30.53)$, $(-40, -40.18)$, and $(-99.19, 0)$, all expressed in meters. These locations were carefully chosen, assuming a speed of sound of $330m/s$, to ensure that the differential delays between the origin and each sensor are all multiples of the sampling period $1/700$s, thereby avoiding the need to implement fractional delays while generating data for the simulation. The noise power is assumed to be the same at each sensor.

Figures 3 and 4 show the MSAE and mean-square range error (MSRE), defined by $\mathrm{E}(\|\hat{\boldsymbol{\theta}}\| - \|\boldsymbol{\theta}\|)^2$, of the location estimated for both the basic WLS estimator and the reweighted estimator, versus the SNR at the origin. A total of 350 snapshots were used, corresponding to a half second observation window during which time the source was supposed to have been approximately stationary. At each SNR 500 realizations were computed. Unsurprisingly, both MSAE and MSRE decrease as SNR increases, however, the estimated bearing is rather more accurate than the estimated range. The standard deviation of the angular error is only $3.5°$ even at 0dB and falls below $1°$ by about 13dB, whereas the standard deviation of the range error is about 23m (about 30% if its distance from the origin) at 0dB. It too however is less than 5m by 15dB and is fractions of a meter at large SNR. It is intuitive that a small error in the local bearings will cause a larger error in the estimated range than in the estimated bearing especially the source the very far from the sensors. Hence the somewhat smaller angular errors, relative to range errors, seen in the simulation. Indeed, it is known that the CRB on range for a passive sensor array is known to increase as the fourth power of the range [35].

The reweighted estimator is seen to provide a slight decrease in both the angular and range error, the improvement is slightly greater for the angle, at all SNR's. Given its low computation cost it is probably worth doing, even though the gain is not large.

6   Conclusion

We developed a fast, wideband decentralized processing scheme for 3-D source localization of airborne targets using a distributed array of aeroacoustic vector sensors. The procedure can be applied to a flexible array, in which each soldier or battlefield unit carries a lightweight sensor package, or to a static array of unattended sensors, deployed in an air-drop over hostile territory perhaps. The algorithm requires minimal communication between each sensor and the base so reducing the likelihood of detection in a hostile environment. The algorithm proceeds in two stages, firstly each sensor locally estimates the bearing to the source, using the by calculating intensities. These estimates are then combined using a WLS procedure at a central processor to determine to 3-D location. We showed that performance could be slightly improved by using a reweighted procedure at this second stage. We also calculated a bound on the MSAE of the bearing estimate for each vector sensor and showed that for the most important angles near normal incidence our algorithm was not too far from optimal.

7   Extensions

There are a number of direction in which we will develop the work presented in this paper, including calculation of the CRB for the full array to provide a benchmark for comparison of the global

position estimator and deriving alternative decentralized estimators based on beamforming. Two different schemes can be considered, one in which beamforming is done at each sensor to estimate the local bearings and another in which the central processor is told the covariance matrix of each sensor location, but does not know the cross covariances between locations, and maximizes the sum of the individual spectra. The former requires more computational power to be packed into each package but each local estimate should be a little more accurate than the current scheme. The latter requires minimal computing power at each location, but requires transmission of more data, namely the whole 4×4 covariance matrix instead of the bearing. We will also extend our model to account for differential Doppler shifts and develop tracking algorithms. Finally, we will extend our model to include ground and surface waves that occur when the source is close to the ground, in order to make it applicable to ground targets.

Appendix A

In this appendix we derive the MSAE_b for a single vector sensor located on the ground. The MSAE_b defined by (4.29) is a function of the CRB on azimuth and elevation. Our measurement model for a single sensor is a member of the class of models whose CRB on the direction parameters is given by Theorem 3.1 of [7]. Note that this theorem only requires inversion of a 2×2 matrix (when applied to our case) even though there are four unknowns as it uses a technique of concentrating the CRB with respect to nuisance parameters developed in [33]. For the current model we obtain

$$\text{CRB}(\phi, \psi) = \frac{1}{2N\rho} \left(1 + \frac{1}{\rho \|\bm{h}\|^2} \right) \left[\text{Re} \left\{ \left(D^H \left(I - \frac{\bm{h}\bm{h}^H}{\|\bm{h}\|^2} \right) D \right)^T \right\} \right]^{-1}, \tag{A.1}$$

where $D = [\partial \bm{h}/\partial\phi, \partial \bm{h}/\partial\psi]$.

Now, from the definition of the vector-sensor steering vector $\bm{h}$ (see (2.11)), noting that the reflection coefficient $\mathcal{R}$ is a function of ψ but not ϕ, we have that

$$\frac{\partial \bm{h}}{\partial \phi} = \begin{bmatrix} 0 \\ -(1 + \mathcal{R}) \sin\phi \cos\psi \\ (1 + \mathcal{R}) \cos\phi \cos\psi \\ 0 \end{bmatrix} \tag{A.2}$$

$$\frac{\partial \bm{h}}{\partial \psi} = \mathcal{R}' \begin{bmatrix} 1 \\ \cos\phi \cos\psi \\ \sin\phi \cos\psi \\ -\sin\psi \end{bmatrix} + \begin{bmatrix} 0 \\ -(1 + \mathcal{R}) \cos\phi \sin\psi \\ -(1 + \mathcal{R}) \sin\phi \sin\psi \\ (1 - \mathcal{R}) \cos\psi \end{bmatrix}, \tag{A.3}$$

where $\mathcal{R}'$ is the derivative of $\mathcal{R}$ with respect to ψ. Now $(\partial\bm{h}^H/\partial\phi)\bm{h} = (\partial\bm{h}^H/\partial\phi)(\partial\bm{h}\partial\psi) = 0$ follows from (A.2) and (A.3), therefore

$$D^H \left(I - \frac{\bm{h}\bm{h}^H}{\|\bm{h}\|^2} \right) D = \begin{bmatrix} \left\| \frac{\partial \bm{h}}{\partial\phi} \right\|^2 & 0 \\ 0 & \left\| \frac{\partial \bm{h}}{\partial\psi} \right\|^2 \end{bmatrix} - \frac{1}{\|\bm{h}\|^2} \begin{bmatrix} 0 & 0 \\ 0 & |(\partial\bm{h}^H/\partial\psi)\bm{h}|^2 \end{bmatrix}, \tag{A.4}$$

and the result (4.30) follows. From (2.11), (A.2), and (A.3) we also obtain the following expressions for the terms involved in MSAE,

$$\|\boldsymbol{h}\|^2 = |1 + \mathcal{R}|^2 (1 + \cos^2 \psi) + |1 - \mathcal{R}|^2 \sin^2 \psi \tag{A.5}$$

$$\left\|\frac{\partial \boldsymbol{h}}{\partial \phi}\right\|^2 = |1 + \mathcal{R}|^2 \cos^2 \psi \tag{A.6}$$

$$\left\|\frac{\partial \boldsymbol{h}}{\partial \psi}\right\|^2 = |1 + \mathcal{R}|^2 \sin^2 \psi + |1 - \mathcal{R}|^2 \cos^2 \psi + 2|\mathcal{R}'|^2 - 4 \operatorname{Re}\{\mathcal{R}'\} \cos \psi \sin \psi \tag{A.7}$$

$$\left|\frac{\partial \boldsymbol{h}}{\partial \psi}^H \boldsymbol{h}\right|^2 = \left|\bar{\mathcal{R}}'\{(1 + \mathcal{R})(1 + \cos^2 \psi) - (1 - \mathcal{R}) \sin^2 \psi\} + (|1 - \mathcal{R}|^2 - |1 + \mathcal{R}|^2) \cos \psi \sin \psi\right|^2, \tag{A.8}$$

where $\bar{\mathcal{R}}'$ indicates the complex conjugate of a $\mathcal{R}'$.

References

[1] D. Lake and D. Keenan, "Maximum likelihood estimation of geodesic subspace trajectories using approximate methods and stochastic optimization," *Proc.9th IEEE SP Workshop on Stat. Sig. and Array Proc.(SSAP),* Portland, OR, Sept. 1998,pp. 148–151.

[2] D. Lake, "Battlefield acoustic signal processing and target identification," web site, URL *http://www.galaxy.gmu.edu/stats/colloquia/colljan3098.html,* George Mason Univ. CSI/Stat. Colloq., Jan 1998.

[3] T. Pham and B. Sadler, "Adaptive wideband aeroacoustic array processing,"*Proc. 8th IEEE SP Workshop on Stat. Signal and Array Process. (SSAP),* Corfu, Greece, June 1996, pp. 295–298.

[4] B.G. Ferguson, "Time-delay estimation techniques applied to the acoustic detection of jet aircraft transits," *J. Acoust. Soc.Am.,* vol. 106, no. 1, pp. 255–264, July 1999.

[5] B.G. Ferguson and B.G. Quinn, "Application of the short-time Fourier transform and the Wigner-Ville distribution to the acoustic localization of aircraft," *J. Acoust. Soc. Am.,* vol. 96, pp. 821–827, 1994.

[6] A. Nehorai and E. Paldi, "Acoustic vector-sensor array processing," *Proc. 26th Asilomar Conf. Signals, Syst. Comput.,* Pacific Grove, CA, Oct. 1992, pp. 192–198.

[7] A. Nehorai and E. Paldi, "Acoustic vector-sensor array processing," *IEEE Trans. on Sig. Proc.,* vol. 42, no. 9, pp. 2481–2491, Sept. 1994.

[8] M. Hawkes and A. Nehorai, "Acoustic vector-sensor beamforming and Capon direction estimation," *IEEE Trans. Signal Processing,*vol. 46, pp. 2291–2304, Sept. 1998.

[9] M. Hawkes and A. Nehorai, "Effects of sensor placement on acoustic vector-sensor array performance," *IEEE J. Oceanic Eng.,* vol. 24, pp. 33–40, Jan. 1999.

[10] K.T. Wong and M.D. Zoltowski, "Closed-form underwater acoustic direction-finding with arbitrarily spaced vector hydrophones at unknown locations," *IEEE J. Oceanic Eng.,* vol. 22, no. 3, pp. 566–575, July 1997.

[11] K.T. Wong and M.D. Zoltowski, "Extended-aperture underwater acoustic multisource azimuth/elevation direction-finding using uniformly but sparsely-spaced vector hydrophones," *IEEE J. Oceanic Eng.*, vol. 22, no. 4, pp. 659–672, Oct. 1997.

[12] G.L. D'Spain and W. S. Hodgkiss, "The simultaneous measurement of infrasonic acoustic particle velocity and acoustic pressure in the ocean by freely drifting swallow floats," *IEEE J. Oceanic Eng.*, vol. 16, no. 2, pp. 195–207, Apr. 1991.

[13] G.L. D'Spain, W. S. Hodgkiss, and G. L. Edmonds, "Energetics of the deep ocean's infrasonic sound field" *J. Acoust. Soc. Am.*, vol. 89, no. 3, pp. 1134–1158, Mar. 1991.

[14] J.C. Nickles et al, "A vertical array of directional acoustic sensors," *Proc. Mast. Oceans thru Tech.(Oceans 92)*, Newport, RI, Oct. 1992, pp. 340–345.

[15] G.L. D'Spain et al, "Initial analysis of the data from the vertical DIFAR array," *Proc. Mast. Oceans thru Tech.(Oceans 92)*, Newport, RI, Oct. 1992, pp. 346–351.

[16] V.A. Shchurov, V.I. Ilyichev, and V.P. Kuleshov, "The ambient noise energy motion in the near-surface layer in the ocean," *Jour. de Physique*, vol. 4, no. 5, part 2, pp. 1273–1276, May 1994.

[17] M. Hawkes and A. Nehorai, "Hull-mounted acoustic vector-sensor array processing," *Proc. 29th Asilomar Conf. Signals, Syst. & Comput.*, pp. 1046-1050, Pacific Grove, CA, Oct. 1995.

[18] M. Hawkes and A. Nehorai, "Surface-mounted acoustic vector-sensor array processing," *Proc. Intl Conf. on Acous.,Speech and Sig. Proc.(ICASSP96)*, pp. 3170–3173, Atlanta, GA, May 1996.

[19] M. Hawkes and A. Nehorai, "Acoustic vector-sensor processing in the presence of a reflecting boundary," submitted to *IEEE Trans. Signal Processing*

[20] B.A. Cray and R.A. Christman, "Acoustic and vibration performance evaluations of a velocity sensing hull array," in *Acoustic Particle Velocity Sensors: Design, Performance and Applications*, (M. J. Berliner and J. F. Lindberg, Eds.), Woodbury, NY: AIP, 1996, pp. 177-188.

[21] R.J. Brind and N.J. Goddard, "Beamforming of a V-shaped array of sea-bed geophone sensors," *J. Acoust. Soc. Am.*, vol. 105, no. 2, pt. 2, pp. 1106, Feb. 1999

[22] Microflown Technologiers, B.V. Netherlands *http://www.microflown.com*.

[23] H.-E. de Bree, P. Leussink, T. Korthorst, H. Jansen, T. Lammerink, and M. Elwenspoek, "The μ-flown: a novel device for measuring acoustic flows," *Sensors and Actuators A*, vol. 54, pp. 552–557, June 1996.

[24] F. van der Eerden, H.-E. de Bree, and H. Tijdeman, "Experiments with a new particle velocity sensor in an impedance tube," *Sensors and Actuators A*, vol. 69, pp. 126–133, Aug. 1998.

[25] P. Stoica, A. Nehorai, and T. Söderström, "Decentralized array processing using the MODE algorithm," *Circ., Syst., and Signal Processing*, vol. 14, no. 1, pp. 17–38, 1995.

[26] M. Wax and T. Kailath, "Decentralized processing in sensor arrays," *IEEE Trans. Acous., Speech, Signal Process.*, vol. 33, no. 4, pp. 1123–1129, Oct. 1985.

[27] A. Nehorai and M. Hawkes, "Performance bounds for estimating vector systems," in revision *IEEE Trans. Signal Process.* A short version appeared in *Proc. Intl Conf. on Acous., Speeh and Sig. Pro. (ICASSP99)*, Phoenix, AZ, March 1999, pp. 1829–1832.

[28] B. Ottersten, M. Viberg, P. Stoica, and A. Nehorai, "Exact and large sample maximum likelihood techniques for parameter estimation and detection in array processing," in *Radar Array Processing* (Ed.: S. Haykin, J. Litva, and T.J. Shepherd), Springer-Verlag: Berlin, 1993, pp. 99–151.

[29] I. Rudnick, "Propagation of an acoustic wave along a boundary," *J. Acoust. Soc. Am.,* vol. 19, no. 1, pp. 348–356, 1951.

[30] A.D. Pierce, *Acoustics—An Introduction to its Physical Principles and Applications.* New York: McGraw-Hill, 1981.

[31] L.M. Brekhovskikh, *Waves in Layered Media*, 2nd Ed. New York, NY: Academic Press, 1980.

[32] S. Haykin *Communications Systems* 2ed., Wiley: New York, NY, 1983.

[33] B. Hochwald and A. Nehorai, "Concentrated Cramér-Rao Bound expressions," *IEEE Trans. Inform. Theory,* vol. 40, no. 2, pp. 363–371, Mar. 1994.

[34] T.F.W. Embleton, J.E. Piercy, and N. Olsen, "Outdoor sound porpagation over ground of finite impedance," *J. Acoust. Soc. Am.,* vol. 59, no. 2, pp. 267–277, Feb. 1976

[35] Y. Rokah, "Array processing in the presence of uncertainty," Ph.D. dissertation, Yale University, Hew Haven, CT, 1986.